To appear in *Engineering Optimization*
Vol. 00, No. 00, Month 20XX, 1–11

Modelling and optimization for a wellhead gas flowmeter using concentric pipes

Yana Nec † and Greg Huculak‡

(*Received 00 Month 20XX; final version received 00 Month 20XX*)

A novel configuration of a landfill wellhead was analyzed to measure flow rate of gas extracted from sanitary landfills. The device provides access points for pressure measurement integral to flow rate computation similarly to orifice and Venturi meters, and has the advantage of eliminating the problem of water condensation often impairing accuracy thereof. It is proved that the proposed configuration entails comparable computational complexity and negligible sensitivity to geometric parameters. Calibration for the new device was attained using a custom optimization procedure, operating on a quadri-dimensional parameter surface evincing discontinuity and non-smoothness.

Keywords: flow rate, landfill gas, flowmeter, Darcy friction factor, optimization on discontinuous surfaces

1. Background

Landfill gas collection often requires installation of flowmeters to comply with environmental regulations. Landfill gas is extracted under vacuum at numerous well points, each monitored for flow rate and gas composition. Methane, carbon dioxide, nitrogen and oxygen are commonly contained in the gas stream extracted. In the past numerous methods have been employed to measure wellhead flow rates: orifice plates, Venturi meters as well as other commercial devices. These devices have been used with some success, however their accuracy is impaired when wet gases are encountered. At times space requirements render their use inappropriate. The geometry of the new device addresses these issues.

The operation principle of an orifice flowmeter is briefly reviewed here to facilitate comparison with the proposed configuration infra. The orifice flowmeter comprises a plate with a centred aperture that is to occlude the fluid conduit, and two sensors to measure the pressure drop due to the occlusion. The flow rate is computed by means of a theoretical formula based on considerations of momentum and supplemented by an empiric discharge coefficient accounting for phyiscal phenomena responsible for head loss not captured by elementary conservation of momentum (Crane 1982). Quondam simplistic models for this coefficient (Idel'chik 1960) proved unsound, the reason thereto designated circa 1980s as a marked sensitivity of orifice calibration to the location of pressure sensors. Since these two entities must be in close conformance to attain adequate accuracy of flow rate estimation, the sensor locations were standardized to a prescribed distance upstream and immediately past the plate, wherewith extensive experiements in conjunction with comprehensive modelling begot the accepted nowadays Reader-Harris / Gallagher dis-

† Thompson Rivers University 900 McGill rd. Kamloops, British Columbia, Canada. Corresponding author. Email: cranberryana@gmail.com

‡ GNH Consulting, Delta, British Columbia, Canada. Email: greg@gnhconsulting.ca

charge coefficient (ISO 2003). However, somewhat cumbersome form thereof and iterative calculation process entailed a praxis of commercial orifice flowmeters being calibrated by the manufacturer in accord with the foregoing principles, providing a formula requiring scarce computational effort, but also delegating the full responsibility for no longer modifiable installation locations of pressure sensors to the field operator.

The following circumstances render the commercial calibration of the orifice flowmeter incompatible with the geometry of a landfill well (Nec and Huculak 2015). In contrast to as universal as it is tacit assumption of horizontal flow used in orifice flowmeters, the well is vertical. Typical flow rates are low, at times necessitating reduction in the aperture diameter to obtain a discernible pressure drop for the measurement, whence momentum loss by gravity is on the same order of magnitude as due to the occlusion by orifice plate. Thus applying a calibration constant issued for a horizontal flow impairs the accuracy of flow rate estimation. Furthermore, it is impossible to instal the second pressure sensor immediately behind the orifice plate due to water vapour, an ever-present component entrained in the landfill gas, condensing thereon. Therefore the pressure sensor locations do not conform to standards. In a recent study adequate accuracy of flow rate estimation was achieved by a custom calibration procedure, incorporating an effective relative roughness parameter to account for turbulence engendered by the presence of the orifice, as well as discovering a linear dependence on the constriction ratio of plate aperture to pipe diameter (Nec and Huculak 2015).

The current contribution proposes a novel wellhead geometry, wherein orifice flowmeter usage is discontinued, eliminating the problem of moisture pooling on the orifice plate and interference with pressure measurement. The new arrangement is shown to be insensitive to imprecision inevitable in field installation, whilst the computational complexity involved in flow rate determination is on par with the custom calibrated orifice flowmeter counterpart (Nec and Huculak 2015). The feasibility of calibration of the new wellhead is verified through a series of measurements, however experiments comprehending the geometric and flow parameter space in its entirety are beyond the ambit of this study.

2. Geometry and flow equations

The wellhead studied herein consists of a tube of inner radius r and wall thickness δ inserted concentrically and secured in a well pipe of radius $R > r$, whose upper end is blocked (see figure 1). The upstream pressure sensor is located by the annulus wall and measures pressure within the nearly stagnant eddy zone. The tube ends with a sharp elbow. A small horizontal recess holds the downstream pressure sensor, measuring the static pressure at that point. The elbow outlet connects to pipework collecting gas from nodes throughout the landfill.

For analysis of mass and momentum balance hereunder consider the control volume from the upstream plane to the elbow inlet plane. Assume the flow steady, axisymmetric and incompressible. Integral mass conservation equation reads (Batchelor 1990)

$$\oint_{\partial V} \rho \mathbf{u} \cdot d\mathbf{s} = 0, \tag{1}$$

with ∂V denoting the surface of the control volume V, ρ being fluid density, $\mathbf{u}$ –velocity vector and $\mathbf{s}$ – area vector with the normal directed outwards. Completing the integration,

$$-\pi R^2 u_{\mathrm{up}} + \pi r^2 u_{\mathrm{i_L}} = 0, \tag{2}$$

wherein u_{up} and $u_{\mathrm{i_L}}$ are upstream and elbow inlet velocities respectively. Defining the

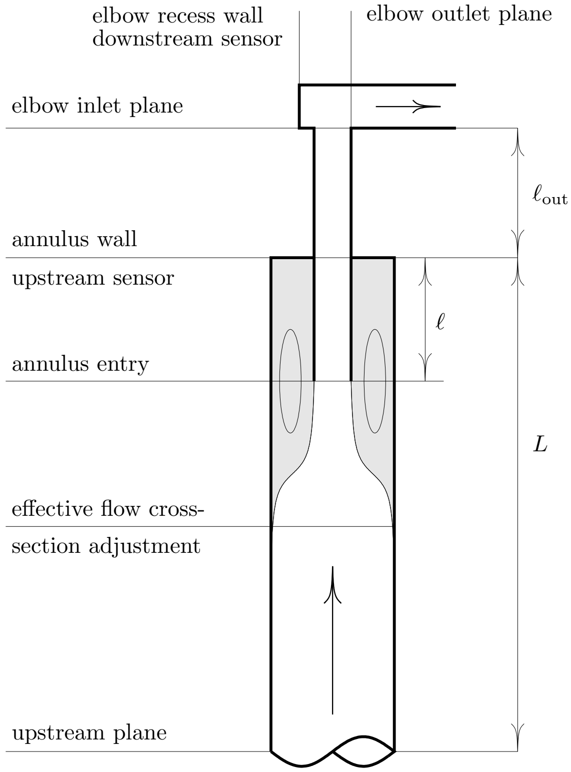

Figure 1.: Wellhead flow geometry. Eddy region is shaded grey.

constriction ratio $\beta = r/R$, equation (2) becomes

$$u_{\mathrm{up}} = \beta^2 u_{\mathrm{i_L}}. \tag{3}$$

Integral momentum conservation equation reads (Batchelor 1990)

$$\int_{\partial V} (\rho \mathbf{u} \cdot d\mathbf{s})\mathbf{u} + \int_{\partial V} p d\mathbf{s} = \int_V \rho\, \mathbf{f}_{\mathrm{body}} dV + \mathbf{f}_{\mathrm{surf}}, \tag{4}$$

with p denoting pressure and $\mathbf{f}_{(\,\cdot\,)}$ – force vectors, remaining quantities defined heretofore. Thus

$$\pi R^2 u_{\mathrm{up}}^2 - \pi r^2 u_{\mathrm{i_L}}^2 + \frac{1}{\rho}\left\{\pi R^2 p_{\mathrm{up}} - \pi\Big(R^2 - (r+\delta)^2\Big)p_{\mathrm{aw}} - \pi\Big((r+\delta)^2 - r^2\Big)p_{\mathrm{ae}} - \pi r^2 p_{\mathrm{i_L}}\right\} = \tag{5}$$

$$g\left\{\pi R^2 L - \pi\ell\Big((r+\delta)^2 - r^2\Big) + \pi r^2 \ell_{\mathrm{out}}\right\} + u_{\mathrm{up}}^2 c_f \Big(\pi R L + \pi(r+\delta)\ell + \pi r(\ell + \ell_{\mathrm{out}})\Big),$$

wherein as before the subscripts $(\,\cdot\,)_{\mathrm{up}}$ and $(\,\cdot\,)_{\mathrm{i_L}}$ refer to upstream and elbow inlet planes, and $(\,\cdot\,)_{\mathrm{aw}}$ and $(\,\cdot\,)_{\mathrm{ae}}$ designating respectively annulus wall and entry planes. Observe that the outlet area of the control volume is threefold: annulus wall, tube wall ring and tube interior, responsible for the negative terms within the first set of braces. Gravity is the sole body force, g denoting the gravity constant, the second set of braces containing the volume of fluid within the pipe and tube compound, with the lengths $L, \ell, \ell_{\mathrm{out}}$ marked in figure 1. The surface force accounts for wall shear, by dimensional analysis equalling a product of dynamic pressure $\frac{1}{2}\rho u_{\mathrm{up}}^2$, friction coefficient c_f and area affected thereby. Without loss of generality u_{up} is a representative velocity for the purpose of friction modelling, whence c_f is in accord with that choice.

The pressure immediately beneath the tube ring is related to the pressure at the annulus wall through a simple fluid column, since both values are for stagnant fluid:

$$p_{\mathrm{ae}} = p_{\mathrm{aw}} + \rho g \ell, \tag{6}$$

allowing to replace p_{ae} in (5) and simplify, yielding

$$u_{\mathrm{up}}^2 - \beta^2 u_{\mathrm{i_L}}^2 + \frac{1}{\rho}\Big(p_{\mathrm{up}} - \big(1-\beta^2\big)\, p_{\mathrm{aw}} - \beta^2 p_{\mathrm{i_L}}\Big) = \tag{7}$$

$$g\Big(L + \beta^2 \ell_{\mathrm{out}}\Big) + u_{\mathrm{up}}^2 c_f \left\{ \frac{L}{R} + \left(\beta + \frac{\delta}{R}\right)\frac{\ell}{R} + \beta\left(\frac{\ell}{R} + \frac{\ell_{\mathrm{out}}}{R}\right)\right\}.$$

The brace delimited term in (7) will infra prove essential to support the negligible sensitivity of the studied flow geometry to variations of ℓ and ℓ_{out}, two parameters prone to installation imprecision.

Identical considerations of mass and momentum in conjunction with dimensional analysis allow to introduce the head loss coefficient ζ_p due to a projection of one concentric conduit within another

$$p_{\mathrm{up}} - p_{\mathrm{i_L}} = \frac{1}{2}\rho u_{\mathrm{i_L}}^2 \left(1-\beta^2\right)\zeta_p + \rho g (L + \ell_{\mathrm{out}}). \tag{8a}$$

Empiric studies show ζ_p to depend on thickness ratio δ/r (Idel'chik 1960). Analogously for a flow through a sharp elbow with a recess

$$p_{\mathrm{i_L}} - p_{\mathrm{o_L}} = \frac{1}{2}\rho\, u_{\mathrm{i_L}}^2\, \zeta_{\mathrm{L}}, \tag{8b}$$

wherein the subscript $(\,\cdot\,)_{\mathrm{o_L}}$ refers to elbow outlet plane, with the head loss coefficient ζ_{L} being a function of relative roughness of the tube inner surface ε and Reynolds number (Idel'chik 1960). Hereunder qualitative use only is made of the dimensionless coefficients ζ_p and ζ_{L}, rendering the accuracy and reproducibility of the specific values given in Idel'chik (1960) of little moment. Since (8b) captures the head loss due to the presence of the sharp bend alone, for all practical purposes $p_{\mathrm{o_L}} = p_{\mathrm{r_L}}$, to wit the pressure measured in the recess $p_{\mathrm{r_L}}$ might be without loss of generality be deemed equal to $p_{\mathrm{o_L}}$, the possible differences absorbed in ζ_{L}. Combining (8a) and (8b) with (3) gives

$$p_{\mathrm{up}} = p_{\mathrm{r_L}} + \frac{\rho u_{\mathrm{up}}^2}{2\beta^4}\left(\left(1-\beta^2\right)\zeta_p + \zeta_{\mathrm{L}}\right) + \rho g\Big(L + \ell_{\mathrm{out}}\Big). \tag{9a}$$

Similarly from (8b) and (3)

$$p_{\mathrm{i_L}} = p_{\mathrm{r_L}} + \frac{\rho u_{\mathrm{up}}^2}{2\beta^4}\,\zeta_{\mathsf{L}}. \tag{9b}$$

Utilizing (9) to replace p_{up} and $p_{\mathrm{i_L}}$ in (7), upon elementary algebraic manipulation one obtains

$$\frac{u_{\mathrm{up}}^2}{2\beta^4}\,C = \frac{p_{\mathrm{aw}} - p_{\mathrm{r_L}}}{\rho} - g\ell_{\mathrm{out}}\,, \tag{10}$$

wherein the coefficient C formally equals

$$C = \zeta_p + \zeta_{\mathsf{L}} - 2\beta^2 - \frac{2\beta^4 c_f}{1-\beta^2}\left\{\frac{L}{R} + \beta^2\left(\left(2 + \frac{\delta}{r}\right)\frac{\ell}{r} + \frac{\ell_{\mathrm{out}}}{r}\right)\right\}. \tag{11}$$

Expression (11) establishes negligibility of geometric minutiae's impact on the hydraulic resistance coefficient C, as is easily seen from the ascending powers of β, the leading order given by ζ_p and ζ_{L}, both $\mathcal{O}(1)$. Interestingly, only even powers of β appear. Since $0 < \beta < 1$, the power of β^6, for instance, implies that the variation of ℓ and ℓ_{out} must be $\mathcal{O}\left(\beta^{-6}\right)$ for that term to bear on the value of C, incontrovertibly exceeding conceivable adjustments made in the course of installation and operation manyfold. This insensitivity renders the reliability of the flow rate to be derived from (10) hereinafter preferable to that of the corresponding orifice estimate evincing marked sensitivity to the location of the pressure gauges. Here the locations are such as to make incorrect installation virtually impossible, involving no measurements and none of the deftness and experience required for an orifice. Therefore only the qualitative dependence $C\,(\beta, \varepsilon, \mathrm{Re})$ is of import, akin to the Reader-Harris / Gallagher discharge coefficient for the orifice (ISO 2003) and the modified coefficient developed in Nec and Huculak (2015).

From (10)

$$u_{\mathrm{up}} = \frac{\sqrt{2}\,\beta^2}{\sqrt{C}}\sqrt{\frac{p_{\mathrm{aw}} - p_{\mathrm{r_L}}}{\rho} - g\ell_{\mathrm{out}}}\,, \tag{12}$$

yielding the volumetric flow rate

$$q = \frac{\sqrt{2}\,\pi r^2}{\sqrt{C}}\sqrt{\frac{p_{\mathrm{aw}} - p_{\mathrm{r_L}}}{\rho} - g\ell_{\mathrm{out}}}\,. \tag{13}$$

Invoking the state equation for ideal gas $p = \rho\mathfrak{R}T$, where $\mathfrak{R}$ and T refer to gas constant and temperature respectively, juxtaposition of (13) above and result (13) of Nec and Huculak (2015) forthwith reveals the conceptual equivalence of the orifice flowmeter and wellhead geometry suggested herein. Identically for both devices the gravity term is negligible by comparison to the pressure drop term for high flow rates, becoming coequal only for nearly stagnant wells.

Albeit the suitability of the geometry analyzed here might not appear surprising given that the wellhead has been ideated with the distinctive features of the landfill flow regime in mind, whilst the orifice is a generic device, to attain its full potential, formula (13) must be furnished with an adequate calculation procedure for the hydraulic resistance coefficient C. Hence it is the authors' intention to glean the qualitative form of $C(\beta, \varepsilon, \mathrm{Re})$, ascertain the feasibility of calibration and verify that overall computational complexity does not exceed that existing for related models of similar accuracy.

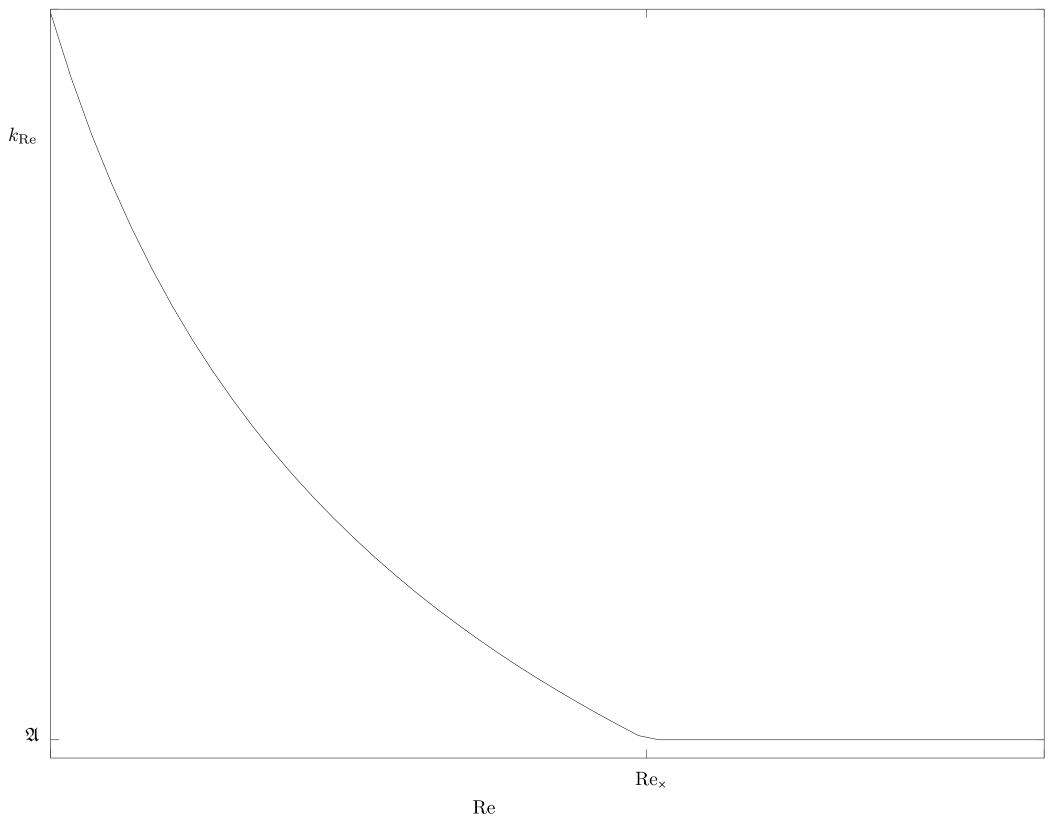

Figure 2.: Typical functional shape of $k_{\mathrm{Re}}(\mathrm{Re})$.

3. Functional form of C

By (11) the resistance coefficient is a function of head loss coefficients ζ_p and $\zeta_{\mathsf{L}}(\varepsilon, \mathrm{Re})$, as well as the constriction ratio β and parameters pertaining to longitudinal geometry together with the friction factor c_f. Bearing in mind that formally $0 < \beta < 1$ and in praxis $0 < \beta < \frac{1}{2}$, identically to the orifice, retainment of terms with powers higher than square is incongruent with the measurement precision expected for the pressure difference in (13). The generic friction factor c_f is of the same order of magnitude as, for instance, Darcy friction factor f (Moody 1944), and for the case of a simple pipe flow can be shown to equal $c_f = \frac{1}{4} f$ (Nec and Huculak 2016). Therefore $c_f \sim o(1)$ and expression (11) is henceforth curtailed to read

$$C = \zeta_p + \zeta_{\mathsf{L}} - 2\beta^2 + o\left(\beta^4\right). \tag{14}$$

The qualitative dependence of ζ_p and $\zeta_{\mathsf{L}}(\varepsilon, \mathrm{Re})$ is adopted from empiric studies (Idel'chik 1960) and consequently modified below to suit the current application.

3.1 *Coefficient* ζ_p

The head loss coefficient ζ_p accounts for the disturbance to flow in the main pipe due to projection of the inner tube thereinto. In general ζ_p depends on the projection length

ℓ/r as well as the thickness ratio δ/r, however for sufficient δ/r the dependence becomes trivial (Idel'chik 1960, pg. 98), as is indeed the case here with $0.1 < \delta/r < 0.2$. Therefore henceforward ζ_p is regarded a constant.

3.2 *Coefficient* $\zeta_{\mathsf{L}}(\varepsilon, \mathrm{Re})$

The head loss coefficient ζ_{L} pertains to the abrupt change in flow direction at the well-head outlet, its two arguments being relative roughness of the conduit material and Reynolds number, here ranging $5{\times}10^{-5} < \varepsilon < 20{\times}10^{-5}$ and $10^4 < \mathrm{Re} < 10^5$ respectively. The functional dependence of ζ_{L} comprises three parts (Idel'chik 1960, pg. 215, table 6-11): generic constant, factor due to Re and factor due to ε:

$$\zeta_{\mathsf{L}} = c\, k_{\mathrm{Re}} k_\varepsilon. \tag{15}$$

The quantitative dependence thereof as given in Idel'chik (1960) is as follows. The parameter k_{Re} is defined by

$$k_{\mathrm{Re}} = \begin{cases} 45f & \mathrm{Re} < 40000 \\ 1 & \mathrm{Re} \geqslant 40000 \end{cases}, \tag{16a}$$

where f refers to Darcy-Weisbach friction coefficient, for a fully turbulent regime obtained by solution of Colebrook equation (Colebrook 1939)

$$\frac{1}{\sqrt{f}} = -2\log_{10}\left(\frac{\varepsilon}{3.7} + \frac{2.51}{\mathrm{Re}\sqrt{f}}\right). \tag{16b}$$

In (16a) the numeric factor 45 is interlocked with the cross-over Reynolds number 40000, so that the curve $k_{\mathrm{Re}}(\mathrm{Re})$ is a continuous function, but non-differentiable at the cross-over point. A typical dependence is shown in figure 2. It is desired to preserve the aforesaid functional dependence whilst converting all fixed empiric constants into variables open to optimization. Therefore definition (16a) is generalized as

$$k_{\mathrm{Re}} = \begin{cases} \mathfrak{A}\dfrac{f}{f_\times} & \mathrm{Re} < \mathrm{Re}_\times \\ \mathfrak{A} & \mathrm{Re} \geqslant \mathrm{Re}_\times \end{cases}, \tag{17a}$$

wherein $\mathfrak{A}$ supplants unity in (16a) and $f_\times$ maintains continuity of k_{Re} through the solution to Colebrook equation with $\mathrm{Re}_\times$:

$$\frac{1}{\sqrt{f_\times}} + 2\log_{10}\left(\frac{\varepsilon}{3.7} + \frac{2.51}{\mathrm{Re}_\times\sqrt{f_\times}}\right) = 0. \tag{17b}$$

For the geometry at hand $\mathrm{Re}_\times$ is expected to be lower than in (16a) due to turbulence engendered by the projecting tube before the bend in flow within the elbow, begetting an earlier cross-over. Furthermore, with the introduction of $\mathfrak{A}$ in (17a) the multiplicative constant c in (15) is to be set to equal unity without loss of generality.

The most general functional form of k_ε is given by

$$k_\varepsilon = \begin{cases} 1 & \mathrm{Re} < \mathrm{Re}_\times \\ 1 + A_\varepsilon \varepsilon & \mathrm{Re} \geqslant \mathrm{Re}_\times \end{cases}. \tag{18}$$

In Idel'chik (1960) the nominal value of A_ε, corresponding to $\mathrm{Re}_\times = 40000$, is $A_\varepsilon = 500$, however here A_ε is a degree of freedom.

In light of the generalizations above four parameters are to be determined before the computation of resistance coefficient C in (14) can be effected: $\zeta_p, \mathfrak{A}, \mathrm{Re}_\times, A_\varepsilon$. This quadruple is obtained infra by minimization of a cost function based on a set of independent measurements.

4. Optimization

The optimization centres on fitting the four variables spanning the parameter space of C with the purpose to show that given a set of trustworthy flow rate measurements, calibration of C can be effected with the stated functional forms for ζ_p and ζ_L. Mathematically, taking a set of measured flow rates $\{q_\mathrm{m}\}$ and corresponding estimates $\{q\}$ as computed by (13), find a set of parameters $\left\{\zeta_p, \mathfrak{A}, \mathrm{Re}_\times, A_\varepsilon\right\}$ such that the norm $\|q - q_\mathrm{m}\|_n$ is minimal, n designating the norm's exponent (solved here for $n = 1$ and $n = 2$ with qualitatively similar results):

$$\min \|q - q_\mathrm{m}\|_n \tag{19a}$$

$$\text{s.t.:} \quad q = \frac{\sqrt{2}\pi r^2}{\sqrt{C}} \sqrt{\frac{p_\mathrm{aw} - p_{\mathrm{r_L}}}{\rho} - g\ell_\mathrm{out}}\,, \tag{19b}$$

$$C\big(\zeta_p, \mathfrak{A}, \mathrm{Re}_\times, A_\varepsilon; \varepsilon, \beta\big) = \zeta_p + \zeta_\mathsf{L} - 2\beta^2, \qquad \zeta_\mathsf{L} = \begin{cases} \mathfrak{A}\dfrac{f}{f_\times} & \mathrm{Re} < \mathrm{Re}_\times \\ \mathfrak{A}(1 + A_\varepsilon \varepsilon) & \mathrm{Re} \geqslant \mathrm{Re}_\times \end{cases} \tag{19c}$$

$$\zeta_p, \mathfrak{A}, \mathrm{Re}_\times, A_\varepsilon > 0.$$

This problem is unusual from several aspects, the combination thereof compounding the complexity of what at first glance might appear an easily amenable task. First, one of the optimization variables, the cross-over Reynolds number $\mathrm{Re}_\times$, is interlocked with the estimate q by a doubly implicit relation: the computation of each estimate point in the set q requires the hydraulic resistance coefficient C that depends on the flow Reynolds number Re, which depends on q by

$$\mathrm{Re} = \frac{4q\rho}{\pi\mu d}, \tag{20}$$

and furthermore the discontinuity point of C is exactly $\mathrm{Re}_\times$, meaning that for any tested value of $\mathrm{Re}_\times$ it is unknown beforehand whether $\mathrm{Re} < \mathrm{Re}_\times$ or $\mathrm{Re} \geqslant \mathrm{Re}_\times$. Second, C is a function of four variables, the quadruple of optimization parameters, but also depending on two parameters ε and β. The relative roughness ε can be deemed fixed, as the pipe material is not expected to change during the optimization procedure. By contrast, the diameter ratio β, whilst fixed for a given geometric configuration, must perforce change for wellheads of different typical flow rates. For a sound accuracy the pressure term $\big(p_\mathrm{aw} - p_{\mathrm{r_L}}\big)/\rho$ in (19b) must significantly exceed the gravity term $g\ell_\mathrm{out}$, thence for an individual well the geometry might be adjusted depending on the gas production: for high flow rates β can be as high as moiety, whilst low flow rates might necessitate $\beta < \frac{1}{6}$. This means that the four arguments of C in (19c) all depend on β. Thence the minimum in (19a) attained upon solution is in fact β-dependent. In this light, an additional, difficult to quantify constraint regards the possible solutions $\left\{\zeta_p, \mathfrak{A}, \mathrm{Re}_\times, A_\varepsilon\right\}$: it is undesirable to have the order of magnitude of these quantities vary significantly with β, albeit a smooth or even monotonic dependence is not expected due to possibly qualitatively different turbulent flow regimes. Unreasonable variation, for instance over several orders of magnitude, is an indicator the physical modelling is wanting. Third, although (19) appears conceptually to be a classic curve fitting problem, it is not: the flow rate q depends explicitly on the pressure difference, but also on temperature T through the density ρ. The viscosity μ that affects Re also depends on temperature. In reality the measurements $\{q_\mathrm{m}\}$ are taken at different temperatures as well. Therefore there is no curve in the classic sense: the available data correspond to disjoint points on a multivariable surface q with an explicit dependence on T through ρ, and an implicit one through Re. One might argue that a carefully controlled experiment will permit to maintain a fixed temperature, however since this model is to be used in reality, artificially controlling the temperature will nullify the applicability of the results of this experiment: then the optimization will only be valid for the particular sub-space conforming to the chosen temperature out of the entire physical parameter space.

Problem (19) is at an obvious variance with studies dedicated to provision of consistent experimental data and subsequent comprehensive modelling (e.g. Colebrook equation for Darcy friction factor and Reader-Harris / Gallagher discharge coefficient for orifice flow rate). Therefore the authors forbear to explore the physical parameter space and focus in lieu on flow regimes characteristic to a landfill, whose field data are summarily accessible (courtesy of GNH Consulting, British Columbia).

Problem (19) was solved by an adaptation of a golden ratio search algorithm to handle the implicit nature, discontinuity and non-smoothness of the involved functions. The search procedure was run on the following part of the parameter space

$$\left\{\zeta_p, \mathfrak{A}, \mathrm{Re}_\times, A_\varepsilon\right\}: \; 0 < \zeta_p < 1, \quad 0 < \mathfrak{A} < 1.5, \quad 10^3 < \mathrm{Re}_\times < 10^5, \quad 100 < A_\varepsilon < 10^4. \qquad (21)$$

A series of local minima of (19a) were stored as the search progressed. None of these were close to the bounds (21). As the bounds were set based on physically meaningful quantities, it is unlikely the global minimum is situated outside (21). The constraint that optimal values be of similar magnitude was exercised only upon completion of the entire search. The existence of numerous local minima is discussed hereinafter.

Although some problems incorporating non-smooth functions are nonetheless amenable to reformulations that permit application of gradient based algorithms, it is conjectured that here this will be impossible due to the implicit nature of the constraints that further compounds the inherent discontinuity.

4.1 *Numerical considerations*

The computation of flow rate q in (13) is iterative: the hydraulic resistance coefficient C depends on Re, whilst Re depends on q by equation (20). Therefore q is estimated by (13) with an initial guess for C, followed by determination of Re from (20), then repeated recomputation of C, q and Re until proper convergence[1]. The optimization was implemented in GNU Octave (open source software), utilizing the function *fminbnd*. For

[1]This is identical to the procedure for an orifice, where Reader-Harris / Gallagher discharge coefficient is employed.

each suggested quadruple $\zeta_p, \mathfrak{A}, \mathrm{Re}_\times, A_\varepsilon$ the hydraulic resistance coefficient C must be converged.

The product of non-differentiable k_{Re}, equation (17a), and discontinuous k_ε, equation (18), renders ζ_{L} a function discontinuous in Re, the selfsame variable that creates the implicit dependence of C on q. The discontinuity point is $\mathrm{Re}_\times$, one of the degrees of freedom in the optimization. This intricate inter-dependence poses certain numerical complications, the most notable being dearth of convergence of C if the Reynolds number is close to the discontinuity point. Even when the likelihood to obtain in the course of the iterative computation of C the singular equality $\mathrm{Re} = \mathrm{Re}_\times$, minuscule as it might be, is eliminated entirely by a negligible shift wheresoever necessary, Reynolds numbers falling sufficiently close to $\mathrm{Re}_\times$ occasion toggling between the two branches of the discontinuous function. When the computation of C does not require evaluation of ζ_{L} on both sides of $\mathrm{Re}_\times$, the convergence to precision of 10^{-6} is obtained within 3-6 iterations, on par with Reader-Harris / Gallagher discharge coefficient that converges to said precision in 2-5 iterations (Nec and Huculak 2015).

A further concomitant of the discontinuity of ζ_{L} is related to the optimization, but will not affect the estimation of flow rate upon completion thereof. It was found that the parameter space spanned by the quadruple $\left\{\zeta_p, \mathfrak{A}, \mathrm{Re}_\times, A_\varepsilon\right\}$ offered multiple local minima to the cost function (19a), when the fit against a set of independent measurements $\{q_{\mathrm{m}}\}$ was performed. Interestingly, designating as a global optimum the quadruple $\left\{\zeta_p, \mathfrak{A}, \mathrm{Re}_\times, A_\varepsilon\right\}_{\mathrm{opt}}$ that gives minimal error, there exist several disparate quadruples $\left\{\zeta_p, \mathfrak{A}, \mathrm{Re}_\times, A_\varepsilon\right\}_{\mathrm{loc}}$ that correspond to local minima with negligibly higher error. This means the field operator will be at liberty to choose any one set of parameters without introducing perceptible inaccuracy into the estimation of flow rate. This situation is unlikely in the extreme with a continuously differentiable multi-dimensional surface underlying the optimization and is the direct outcome of the discontinuity in (18) and non-smoothness in (17a).

4.2 *Results*

Three flow regimes were considered: high flow rate engendered by an active well, medium flow rate corresponding to moderate production and low flow rate conforming to a slowly producing well. In all cases a set of reliable measurements $\{q_{\mathrm{m}}\}$ was chosen so as to span as uniformly as possible the concomitant interval of differential pressure. The optimization was performed separately, verifying the combined results presented a physically acceptable solution. Figures 3-5 depict the comparison between the measured flow rate and estimate (13) with $\left\{\zeta_p, \mathfrak{A}, \mathrm{Re}_\times, A_\varepsilon\right\}_{\mathrm{opt}}$.

When a well is active, a typical constriction ratio is $\beta \approx \frac{1}{3}$ with ensuing Reynolds numbers ranging $10^4 < \mathrm{Re} < 6{\times}10^4$. The corresponding cross-over Reynolds number $\mathrm{Re}_\times$ is relvatively low, whereby for most of the working range the hydraulic resistance coefficient C is constant, entailing a rapid convergence. When the Reynolds number is close to $\mathrm{Re}_\times$, it will behove the operator to adjust the wellhead to a smaller constriction ratio so as to maintain a viable pressure difference. An example of this situation is shown in figure 3.

If gas production within the landfill cavity in the proximity of a well diminishes, the constriction ratio will be reduced to $\beta \approx \frac{1}{4}$ in order to sustain the same working range of Reynolds numbers, this time $\mathrm{Re}_\times$ found in the upper part thereof, again enabling effortless convergence in praxis. Figure 4 details this intermediate flow regime.

For slow production wells the suitable constriction ratio might be as low as $\beta \approx \frac{1}{5}$, with a similar range of Reynolds numbers and $\mathrm{Re}_\times$ falling midmost (figure 5). This is the only regime, where toggling around the discontinuity point is likely to present difficulty. As a rule, higher constriction ratios are preferable as long as the pressure difference is aptly measurable. Therefore a configuration with such low β will be installed for $\mathrm{Re} < \mathrm{Re}_\times$ and changed in favour of a higher β if the cross-over point is approached.

The optimal quadruples $\zeta_p, \mathfrak{A}, \mathrm{Re}_\times, A_\varepsilon$ reported in figures 3-5 corresponded to the global error minimum for each set of reference measurements. Whilst it is possible to choose one of the quadruples conforming to local minima for any particular constriction ratio, only the global optima entail a logical adjustment of flow regimes with the fluctuations in gas production, when the entire spectrum of operation is considered.

5. Conclusion

The novel wellhead configuration presented targeted a long-standing problem of impaired flow rate metering in landfill wells due to condensation of water vapour entrained in the fluid upon the orifice plate and interference with the pressure sensor that must be placed in an immediate proximity thereof. In the proposed setting the fluid proceeds from the main well pipe into a concentric tube of a smaller diameter, permitting to withdraw the orifice plate. The resulting flow rate was proved to be conceptually equivalent to the orifice device by considerations of mass and momentum conservation. The sensitivity of concomitant pressure measurement to installation geometry was shown to be minor, and the associated error was evaluated asymptotically in constriction ratio β, an inherent small parameter of the system.

The hydraulic resistance coefficient was modelled by adopting the functional form of empiric coefficients in related geometries and performing a custom optimization to attain a fit against a set of independent measurements. The optimization involved a quadri-dimensional discontinuous surface with an implcit dependence that required iterative numerical solution. In field use the computational complexity was shown to be on par with devices endowed with similar accuracy of flow rate estimation.

References

Batchelor, G.K. 1990. *Introduction to fluid dynamics.* Cambridge.

Colebrook, C.F. 1939. "Turbulent flow in pipes, with particular reference to the transition region between the smooth and rough pipe laws." *Journal of the Institution of Civil Engineers* 11: 133–156.

Crane, Co. 1982. *Flow of fluids through valves, fittings and pipe. Technical paper No. 410M.* 300 Park Avenue, New York, NY 10022, appendix A-5.

Idel'chik, I.E. 1960. *Handbook of hydraulic resistance. Coefficients of local resistance and of friction (translated from Russian).* Published for US Atomic Energy Commission and NSF, Washington DC, AEC-tr-6630, 1966.

ISO. 2003. "Measurement of fluid flow by means of pressure differential devices inserted in circular cross-section conduits running full - part 2: Orifice plates." .

Moody, L.F. 1944. "Friction factors for pipe flow." *Transactions of ASME* 66: 671–684.

Nec, Y., and G. Huculak. 2015. "On the problem of a vertical gas flow through an orifice with non-standard pressure tappings locations." *Can.J.Civ.Eng.* 42: 563–569.

Nec, Y., and G. Huculak. 2016. "Solution of weakly compressible isothermal flow in landfill gas collection networks." *submitted to Fluid Dynamics Research* .

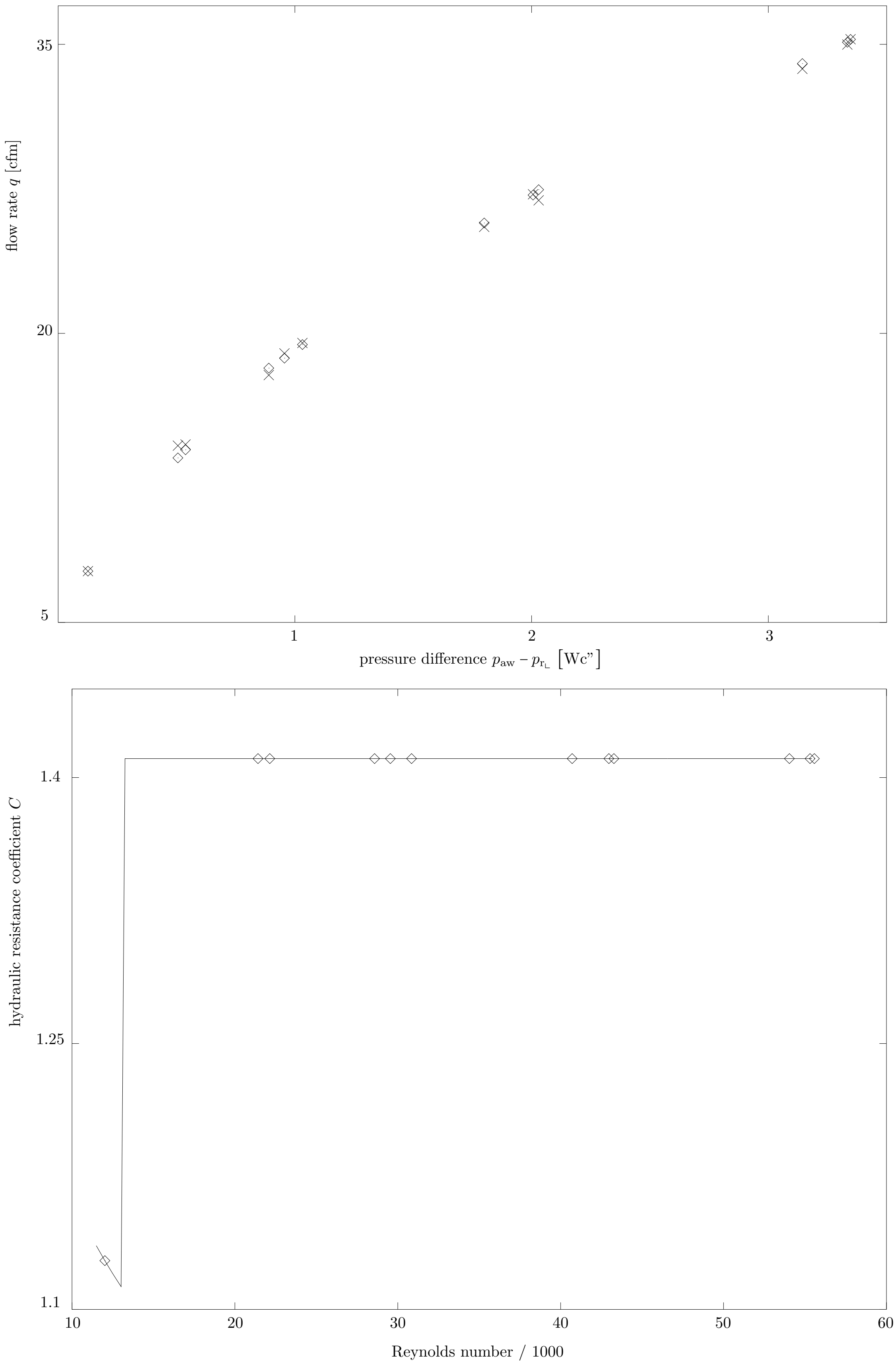

Figure 3.: A typical example of flow regime for $\beta = \frac{1}{3}$. Top: optimization output (diamond) and independently measured (cross) flow rate. Reference points included multifarious values of density ρ, viscosity μ and relative roughness ε, rendering interpolation unfeasible. Bottom: hydraulic resistance coefficient C versus Re. Optimal parameters: $\zeta_p = 0.66$, $\mathfrak{A} = 0.71$, $\mathrm{Re}_\times = 13000$, $A_\varepsilon = 7300$. Diamond symbols on both panels correspond.

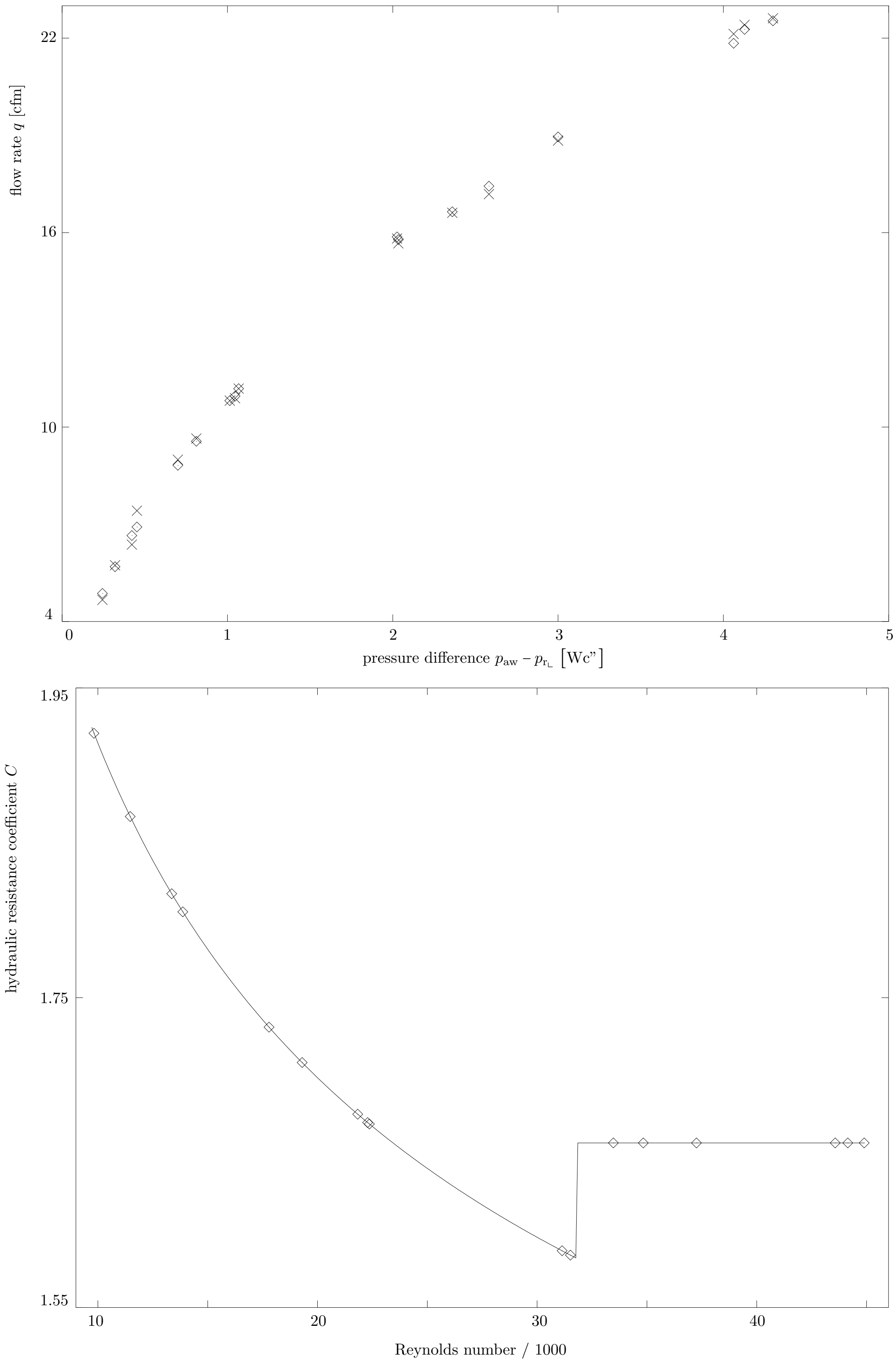

Figure 4.: A typical example of flow regime for $\beta = \frac{1}{4}$. Top: optimization output (diamond) and independently measured (cross) flow rate. Reference points included multifarious values of density ρ, viscosity μ and relative roughness ε, rendering interpolation unfeasible. Bottom: hydraulic resistance coefficient C versus Re. Optimal parameters: $\zeta_p = 0.72$, $\mathfrak{A} = 1.02$, $\mathrm{Re}_{\times} = 31800$, $A_{\varepsilon} = 1000$. Diamond symbols on both panels correspond.

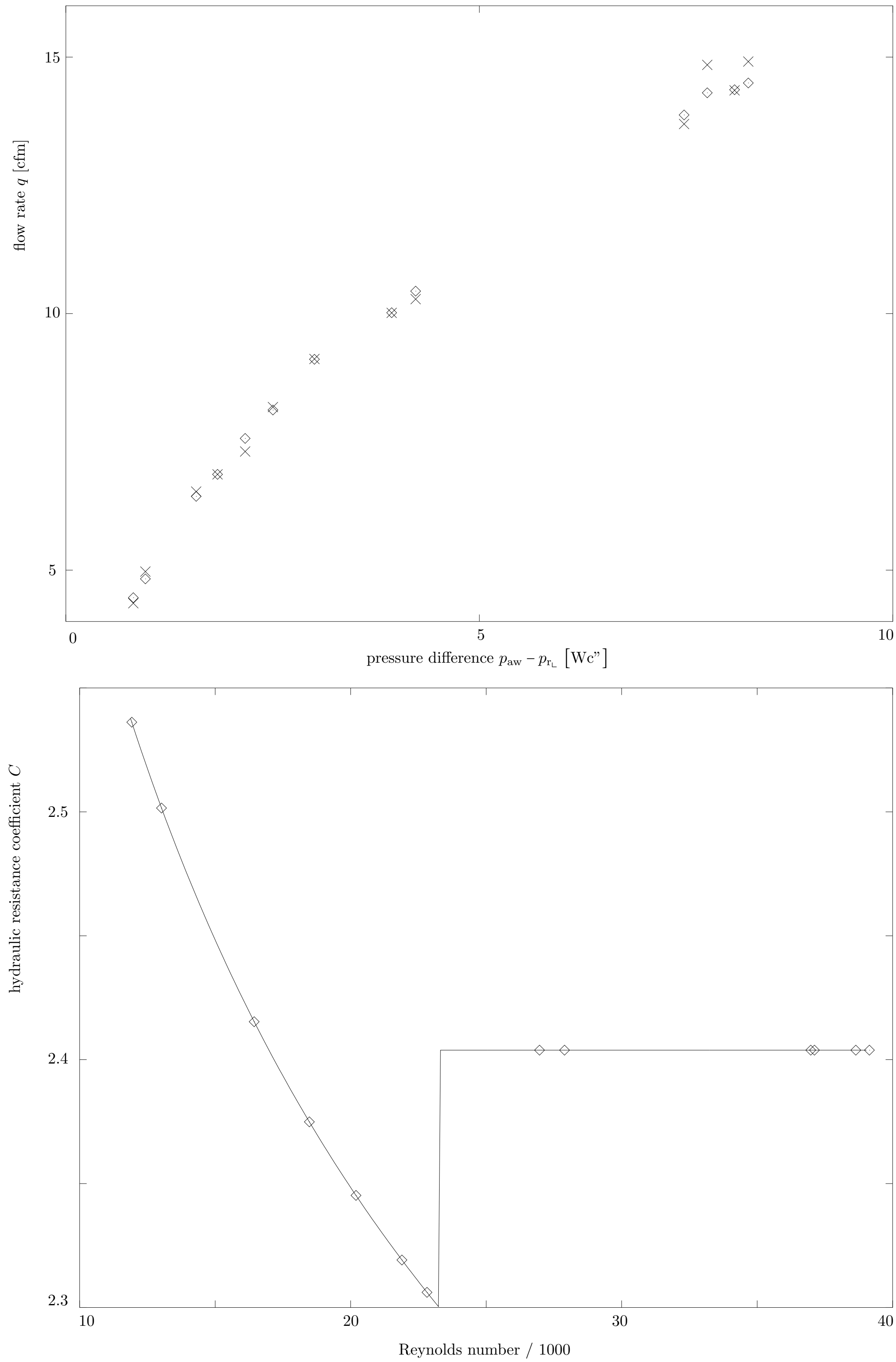

Figure 5.: A typical example of flow regime for $\beta = \frac{1}{5}$. Top: optimization output (diamond) and independently measured (cross) flow rate. Reference points included multifarious values of density ρ, viscosity μ and relative roughness ε, rendering interpolation unfeasible. Bottom: hydraulic resistance coefficient C versus Re. Optimal parameters: $\zeta_p = 1.06$, $\mathfrak{A} = 1.33$, $\mathrm{Re}_\times = 23000$, $A_\varepsilon = 800$. Diamond symbols on both panels correspond.